BMB
reports

The effect of rod domain A148V mutation of neurofilament light chain on filament formation

In-Bum Lee[1,#], Sung-Kuk Kim[1,#], Sang-Hee Chung[1], Ho Kim[1], Taeg Kyu Kwon[2], Do Sik Min[3] & Jong-Soo Chang[1,]*

[1]Department of Life Science, College of Natural Science, Daejin University, Pocheon, [2]Department of Immunology, College of Medicine, Keimyung University, Taegu, [3]Department of Molecular Biology, College of Natural Science, Pusan National University, Busan, Korea

Neurofilaments (NFs) are neuronal intermediate filaments composed of light (NF-L), middle (NF-M), and heavy (NF-H) subunits. NF-L self-assembles into a "core" filament with which NF-M or NF-H co-assembles to form the neuronal intermediate filament. Recent reports show that point mutations of the NF-L gene result in Charcot-Marie-Tooth disease (CMT). However, the most recently described rod domain mutant of human NF-L (A148V) has not been characterized in cellular level. We cloned human NF-L and used it to engineer the A148V. In phenotypic analysis using SW13 cells, A148V mutation completely abolished filament formation despite of presence of NF-M. Moreover, A148V mutation reduced the levels of *in vitro* self-assembly using GST-NF-L (H/R) fusion protein whereas control (A296T) mutant did not affect the filament formation. These results suggest that alanine at position 148 is essentially required for NF-L self-assembly leading to subsequent filament formation in neuronal cells. [BMB reports 2008; 41(12): 868-874]

INTRODUCTION

Neurofilaments (NFs) are the most abundant cytoskeletal components in large myelinated axons and exist as obligated heteropolymers composed of NF-L, NF-M and NF-H (1-3). Each NF is composed of three domains: a N-terminal head domain, an α-helix-rich rod domain, and a C-terminal tail domain (4-6). The head domain regulates filament assembly *via* protein phosphorylation (7-9). The rod domain is responsible for coiled-coil dimer formation, which is an essential step in neurofilament assembly (10). *In vitro* reconstitution studies revealed that NF-L assembles to form core filaments (11), while NF-L alone cannot assemble into the filaments *in vivo* (12-14). Within a cell, NF-L unconditionally requires NF-M or NF-H to form neurofilaments via cross-bridging of NF-L/NF-M and/or NF-L/NF-H (2, 15). Fully formed heteropolymeric neurofilaments composed of NF-L/NF-M and/or NF-L/NF-H are key components of axonal neurites.

Mutations in the human NF-L (*h*NF-L) gene have recently been shown to cause Charcot-Marie-Tooth disease (CMT), which is characterized by demyelination and axonal degeneration of neurons. Among the mutant forms of *h*NF-L linked to CMT are several encoded by missense mutations, including P8L, P8Q, P8R, P22S, P22T, E89K, N97S, A148V, Q333P, L334P and D469N (16-22). With the exception of *h*NF-L-A148V, which has not been tested in cultured cell systems, each of these mutant proteins causes aggregation of *h*NF-L, consistent with the proposed relationship between CMT and point mutations in the *h*NF-L gene. To examine the capability for filament formation by the A148V mutant *in vitro* and *in vivo*, we cloned a human cDNA for wild type NF-L and mutated it to A148V and A296T as a control. Here we demonstrate for the first time that exogenously expressed *h*NF-L- A148V is unable to form filamentous structures in SW13 cells, suggesting that the A148V mutation is also associated with CMT.

RESULTS AND DISCUSSION

Preparation of cDNA for human NF-L

An analysis of cDNA from CMT patients reveals the existence of point mutations in the NF-L gene (Fig. 1A) that cause disassembly of NF-L (16-22). The effect of these mutations on filament assembly has been confirmed by phenotypic analysis of mutant NF-L proteins exogenously expressed in SW13 cells. However, the most recently discovered A148V mutant, which has not been previously characterized, exhibits exception. To facilitate such a phenotypic analysis of the A148V mutation in SW13 cells, we amplified a DNA fragment that matched the expected size of the *h*NF-L coding region using a human rain cDNA library (Fig. 1B). Comparison of the resulting DNA sequence to public database NCBI showed that this product was indeed *h*NF-L, which has a reading frame of 1,632 bp encoding 543 amino acids (Fig. 1C). We have also prepared the corresponding *h*NF-L-A148V mutant construct and verified that the substitution of alanine for valine at position 148 was correctly introduced (Fig. 1C). In our recent study, since substitution of alanine for threonine at position 296 in rod-domain

*Corresponding author. Tel: 82-31-539-1853; Fax: 82-31-539-1850;
E-mail: jchang@daejin.ac.kr
#Lee, I.B. and Kim, S.K. contributed equally to this work

Received 3 June 2008, Accepted 2 July 2008

Keywords: A148V, Charcot-marie-tooth, Neurofilaments, Self-assembly, SW13 cells

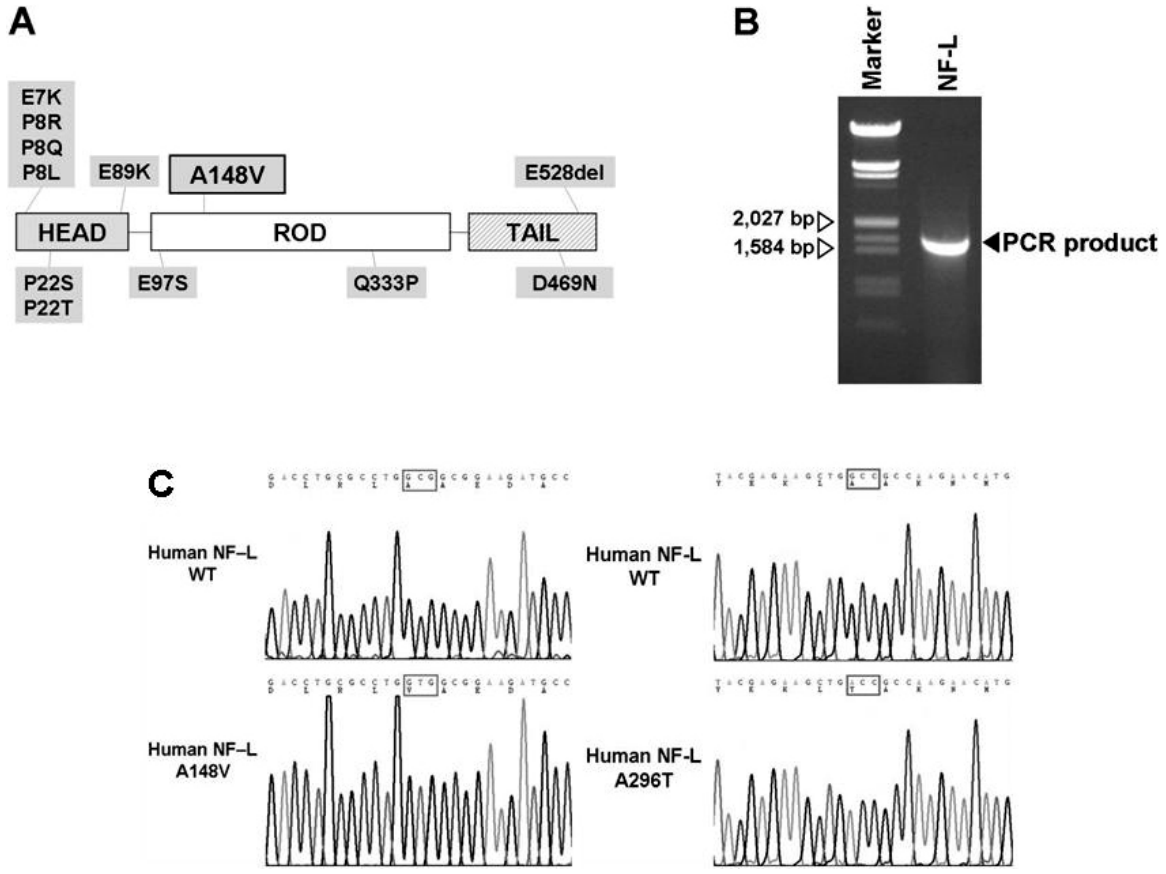

Fig. 1. PCR amplification and sequence analysis of wild-type *h*NF-L, *h*NF-L-A148V and -A296T. (A) NF-L mutations in CMT disease. (B) Amplification of the *h*NF-L gene from a human fetal brain marathon cDNA library using human NF-L-specific primers yields a PCR product of the predicted size. *h*NF-L-A148V and -A296T mutations were prepared by substituting alanine for valine at position 148, and alanine for threonine at position 296 using PCR-directed mutagenesis respectively. (C) Sequences of NF-L wild type and NF-L mutants (A148V and A296T) were confirmed as described in Materials and Methods.

of NF-L did not affect self assembly (data not shown), we used this A296T mutation of NF-L as a negative mutant control for all subsequent experiments.

Phenotypic expression of human NF-L in SW13 cells

Generally, NF-L self-assembles to form a "core" filament that provides a scaffold for NF-M or NF-H, leading to the formation of neurofilaments in most neurons. *In vitro* studies have shown that NF-L self-assembles in the presence of Ca^{2+} but it dose not polymerize to a filamentous form *in vivo* (23). This indicates that *in vivo* filament formation of NF-L requires at least NF-M or NF-H (24). The vimentin-deficient human adrenal carcinoma SW13 cell (25) is a model cell that is permissive for intermediate filament formation upon co-expression of NF-L with NF-M or NF-H (1, 2). As previous reports, SW13 cells transfected with NF-M and NF-L-full (full length)-WT together showed intermediate filament formation but not in cells transfected with NF-L-full-WT alone (Fig. 2A). Based on these results, subsequent experiments for NF-L filament formation were performed in the presence of co-transfected NF-M. We next analyzed the phenotypic expression of the NF-L-full length with a rod domain A148V mutation in SW13 cells. Co-expression of GFP-NF-L-full-WT with Flag-NF-M formed filamentous structures (Fig. 2B). A296T mutation in the rod domain of NF-L, a negative mutation control, also formed typical intermediate filament in SW13 cells. However, the rod domain mutation A148V mutation drastically abolished filament formation despite presence of NF-M, indicating an indispensable function for alanine at position 148 in the formation of structural filaments within neuronal cells. Moreover, this phenotype is similar to that reported for other CMT-linked mutations (18-20, 22). This result also indicates that the A148V mutation may also be closely associated with CMT. Green fluorescence indicating NF-L-full-WT and NF-L-full-mutants (A148V and A296T) completely merged to red color reflecting NF-M subcellular distribution in SW13 cells. Western analysis

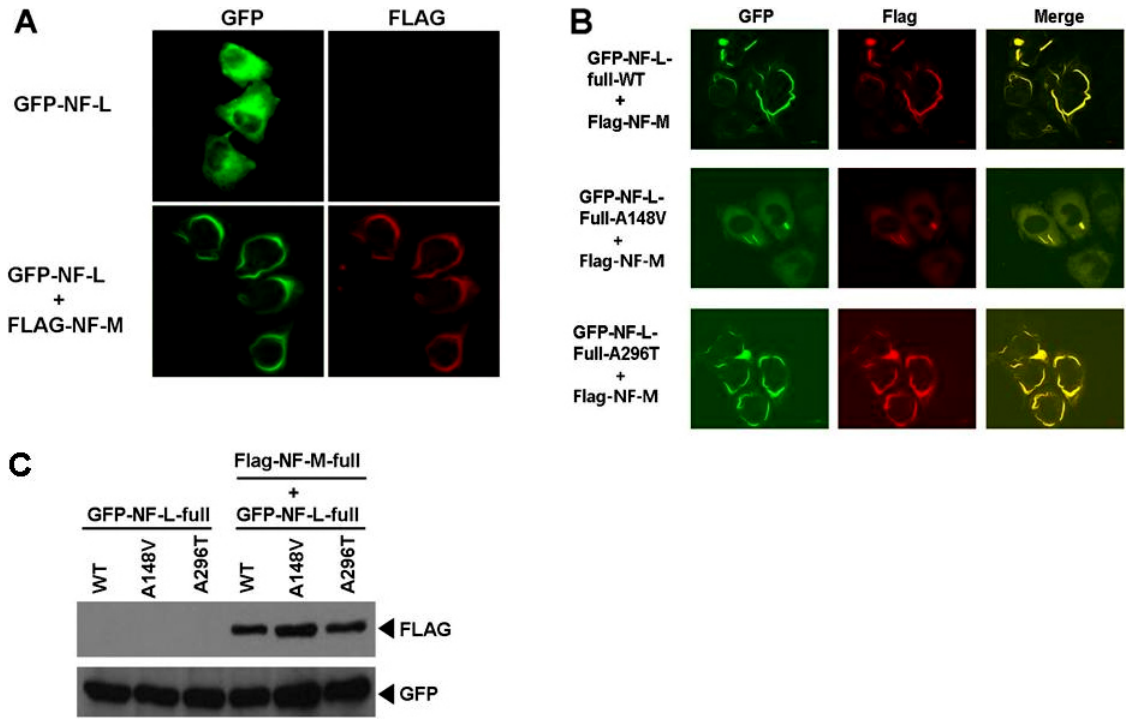

Fig. 2. A148V mutation of NF-L fails to form a heteropolymer with NF-M in SW13 cells. (A) Requirement of NF-M for *in vivo* filament formation of NF-L. SW13 cells (Vim-) grown on glass coverslips were transfected transiently with either GFP-NF-L alone (upper) or GFP-NF-L plus NF-M (bottom). The cells were fixed with 4% paraformaldehyde and filament formation was visualized by fluorescence confocal microscopy. (B) Detection of wild-type NF-L (WT) and mutant NF-Ls (A148V or A296T) to form filamentous structures. SW13 cells (Vim-) grown on glass coverslips were co-transfected with NF-M and either GFP-NF-L-WT (upper), GFP-NF-L-A148V (meddle) or GFP-NF-L-A296T (bottom). NF-M proteins overexpressed in SW13 cells were stained with an antibody against FLAG and followed by rhodamine-conjugated secondary antibodies. (C) NF-M and GFP-NF-L proteins overexpressed in SW13 cells were measured by Western blotting with antibodies against FLAG (upper) or GFP (bottom). The results shown here are representative of 3 individual experiments.

of SW13 cell lysates transfected with the indicated genes confirmed the expression of wild type and mutant NF-Ls as GFP fusion proteins (Fig. 2C, bottom) and the exogenous overexpression of NF-M (Fig. 2C, top).

A148V mutant in rod domain of NF-L abolishes self assembly

We previously reported that head-rod domains of NF-L were sufficient for detecting the levels of self-assembled NF-L and that GST-fused head-rod domains (H/R) of NF-L are critical tools for analyzing NF-L self-assembly *in vitro* (26). Based on this finding, we assessed whether A148V mutation influenced self-assembly of NF-L *in vitro*. To clarify this, GST-NF-L-H/R, GST-NF-L-H/R-A148V and GST-NF-L-H/R-A296T fusion proteins were mixed with *E.coli*-purified full length NF-L (NF-L-full-WT), and incubated for 1 h at 4°C. Associated proteins were recovered by centrifugation, washed extensively, and analyzed by Western immunoblotting. As shown in Fig. 3A, GST-NF-L (H/R) fusion protein clearly bound to NF-L-full-WT (lane 1), whereas this interaction was markedly reduced by substitution of alanine for valine at position 148 in rod domain (lane 1 vs lane 2). In contrast, substitution of alanine for threonine at position 296 (A296T mutant), randomly selected within the NF-L rod domain did not hinder filament formation in SW13 cells, indicating essentiality of alanine at position 148 in rod domain in the NF-L self assembly. Fig. 2B data showing marked disruption on filament formation in SW13 cells transfected with NF-L-full-A148V and NF-M also supports these findings. Expected protein size of purified NF-L-full-WT protein was indicated (lane 1). The graph represents densitometirc Western blotting (lower), and schematic diagrams (left) present data as designated. Purified GST-NF-L-H/ R-A148V proteins were mixed with either *E.coli*-NF-L-full-WT or *E.coli*-NF-L-full-A148V. As expected, addition of NF-L-H/R-A148V to NF-L-full-A148V significantly reduced self-assembly (lane 6), and this is even lower than addition of NF-L-H/R to NF-L-full-A148V (lane 3 vs lane 5, lane 4 vs lane 6), confirming the critical role of A148V mutation on NF-L self-assembly. These results also suggest that CMT-linked point mutations directly affect NF-L self-assembly rather than disrupting interfilament interactions with NF-M or NF-H. Expected protein size and loaded amount of purified *E.coli*-NF-L-full-WT and *E.coli*-NF-L-full-A148V proteins are indicated respectively (Fig. 3B, lanes 1 and 2). The

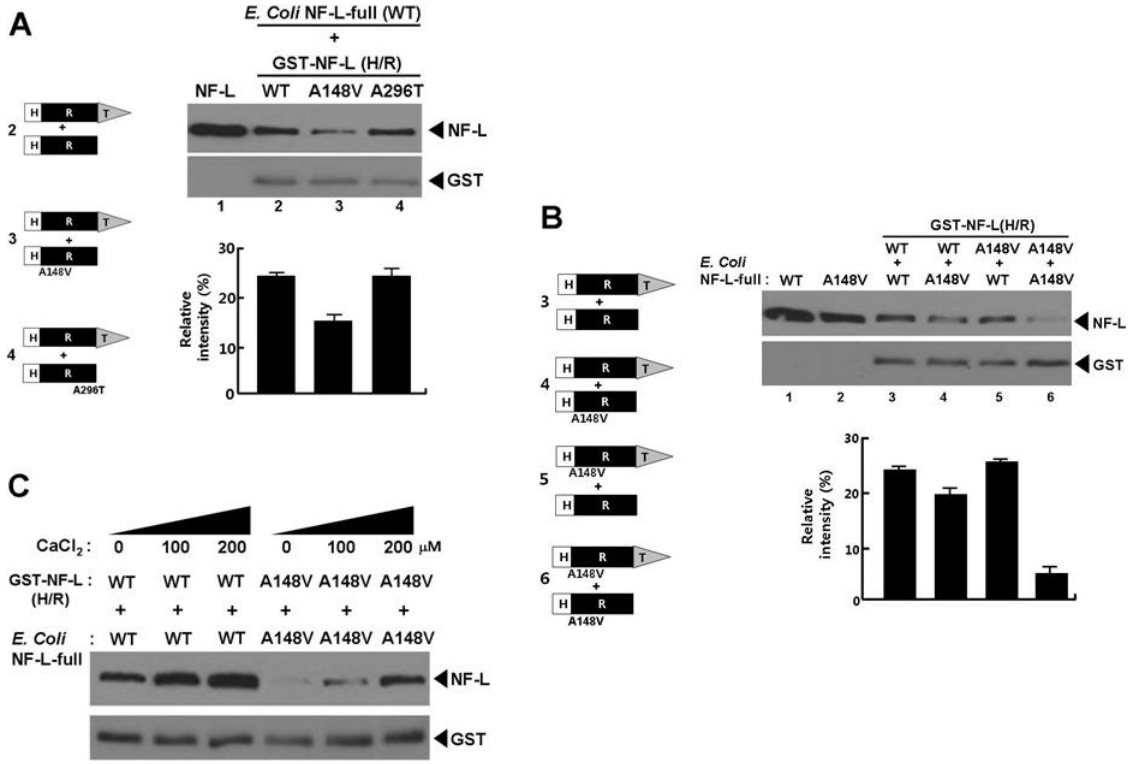

Fig. 3. A148V mutation in rod domain and NF-L-self assembly. (A) *E.coli*-purified full length (full)-NF-L is incubated with either GST-NF-L-H/R (head/rod domain), GST-NF-L-H/R-A148V or GST-NF-L-H/R-A296T fusion proteins for 1 h at 4°C and then the associated proteins recovered by centrifugation. *E.coli*-purified full NF-Ls binding to NF-L-(H/R) or NF-L-(H/R)-mutants were detected by an antibody recognizing carboxyl terminus region of NF-L. Expected size of purified *E.coli*-NF-L-full (WT) protein was indicated (lane 1). Densitometirc western blotting Graph (lower). (B) GST-NF-L-H/R and GST-NF-L-H/R-A148V proteins were mixed with either *E.coli*-full NF-L (WT) or *E.coli*-NF-L-full-A148V respectively and then the associated proteins were detected by NF-L antibody. Expected protein size and loaded amount of purified *E.coli*-NF-L (WT) and *E.coli*-NF-L-A148V proteins were indicated (lanes 1, 2). (C) Ca^{2+} reverses NF-L-A148V mutant reduction of self assembly. Purified *E.coli*-full-NF-L (WT) and *E.coli*-full-NF-L-A148V proteins were incubated with either NF-L-H/R or NF-L-H/R(A148V) fusion proteins for 2 h at 35°C in the presence of Ca^{2+}. Results shown here are representative of 3 individual experiments.

graph represents densitometirc western blotting (lower) and schematic diagrams (left) present designated experiments.

How does the A148V mutant of human NF-L lead to defective filament assembly and the formation of aggregates? Although our experiments do not address this question, in case of P22T and P22S head-domain mutations related to CMT, their mutations have been reported to result in shorter and thinner intertwined filaments versus normally polymerized filaments in an *in vitro* assembly assay (27). Based on the ability of head domain of NF-L to polymerize core filaments (2), the mutation of alanine to valine at position 148 may cause failure of dimerization known to be mediated by coiled coil region in NF-L rod domain (10). Interactions of hydrophobic amino acids have known to form coiled coil dimers in the α-helical rod domain (28). Since alanine and valine are similar, both nonpolar aliphatic residues, and their substitution has no known effect on protein structure (28), A148V mutation may be considered a polymorphism and uninfluential towards production traits. Our findings, that A148V mutation abolished NF-L self assembly as well as *in vivo* filament formation, may also be linked with other unknown mechanism. This hypothesis is likely supported by findings of A117V substitution in prion protein and its link to Gerstmann-Sträussler-Scheinker disease (GSS) of humans, possibly through favoring β-sheet conformation over the α-helical conformation (29). Kirschner *et al* also showed that substitutions of alanine at position 117 with various hydrophobic amino acids did not destabilize the helix conformation, only valine substitution resulted in helix destabilization leading to failure of hydrophobic interactions (30).

Since ionic strength (10, 23) and treatment of Ca^{2+} (26) affects NF-L self assembly, we next investigated the effect of Ca^{2+} on self-assembly by NF-L-WT or NF-L-A148V mutant. Purified *E.coli*-NF-L-full-WT and *E.coli*-NF-L-full-A148V proteins were incubated with NF-L-H/R or NF-L-H/R (A148V) fusion proteins in the presence of Ca^{2+} for 2 h at 35°C. As shown in Fig. 3C, Ca^{2+} treatment increased self assembly in

both *E.coli*-NF-L-full-WT plus NF-L-H/R and *E.coli*-NF-L-full -A148V plus NF-L-H/R-A148V in a dose dependent manner, confirming that Ca^{2+} treatment induces not only the levels of self-assembly of intact NF-L, but also restoring A148V mutation-reduced NF-L self-assembly. It is likely that A148V mutation on the central rod domain of NF-L may fail to dimerize but this can be recovered by Ca^{2+} through mediation of certain conformational changes on the rod domain.

Overexpression of NF-L-A148V mutant in PC12 cells co-expressing NF-M and NF-H

We next investigated the effect of exogenously introduced NF-L-full-A148V mutant on filament formation in PC12 cells that co-express NF-M and NF-H in contrast to SW13 cells which lack these proteins (25). PC12 cells were transfected with GFP-NF-L-full-WT, GFP-NF-L-full-A148V or GFP-NF-L-full-A296T. Filament formations were visualized by fluorescent confocal microscopy. Overexpression of GFP-NF-L-full-WT and GFP-NF-L-full-A296T formed typical intermediate filaments with a fine and continuous network, whereas NF-L-full-A148V mutant overexpression, at least in part, caused smaller and thinner cytoplasmic aggregates than NF-L- WT-cells, although long filamentous networks were observed in most of the transfected cells (Fig. 4). This result suggests that the NF-L-A148V mutant has a dominant negative effect, and it partially blocks self-assembly of endogenous NF-L assembly leading to intermediate filament formation with NF-M and NF-H in PC12 cells.

Taken together, the mutation of alanine to valine at position 148 in human NF-L rod domain abolished assembly into intermediate filaments *in vivo* and reduced self-assembly of NF-L *in vitro*. These results suggest that NF-L- A148V mutation is one of the mutations causing CMT.

MATERIALS AND METHODS

Reagents

Monoclonal (mAb 1615) and polyclonal anti-NF-L antibodies were purchased from Chemicon (Temecula, CA). Monoclonal anti-NF-M antibody (mAb RNF403) used in immunocytochemistry applications was from MP Biochemicals (Aurora, OH). Horseradish peroxidase (HRP)-conjugated goat anti-mouse and goat anti-rabbit antibodies were from Upstate Inc. (Lake Placid, NY). Fluorescein-conjugated Affinipure goat anti-rabbit IgG and rhodamine-conjugated Affinipure goat anti-mouse IgG were from Jackson ImmunoResearch Laboratories (West Grove, PA). PCR reagents were from Roche Diagnostics (Mannheim, Germany) and the human fetal brain marathon cDNA library (Cat # S0623) was purchased from CLONTECH (Palo Alto, CA).

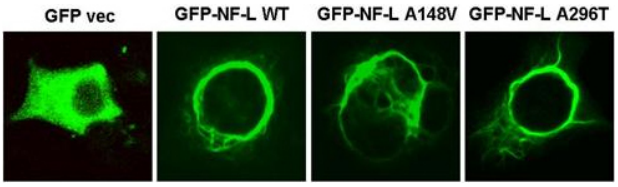

Fig. 4. Inhibitory effect of NF-L-A148V mutant on intermediate filament formation in PC 12 cells expressing NF-L, NF-M and NF-H. PC12 cells grown on glass coverslips were transfected with GFP-vector, GFP-NF-L-WT, GFP-NF-L-A148V and GFP-NF-L-A296T and then intermediate filament formations were visualized by fluorescent confocal microscopy. Results presented here are representative of 3 individual experiments.

PCR cloning

The *h*NF-L gene was amplified from a human fetal brain marathon cDNA library (Clontech) by PCR using the following primers: 5′-GCT *GAA TTC* **ATG** AGT TCC TTC AGC TAC GAG-3′ (forward), and 5′-CAT *GTC GAC* **TCA** ATC TTT CTT CTT AGC TGC-3′ (reverse). Italicized sequences correspond to EcoRI and SalI restriction sites added to the 5′ ends of forward and reverse primers, respectively, to facilitate cloning. The resulting PCR product (1.6 kb) was directionally cloned into EcoRI and SalI sites of the pGEX5x-1 vector (Amersham Pharmacia) to generate a plasmid, designated pGEX5x-1- *h*NF-L, containing the full-length, wild-type *h*NF-L gene. The identity of the gene was confirmed by DNA sequencing.

Site-directed mutagenesis

The mutations of alanine at position 148 to valine and alanine at position 296 to threonine in *h*NF-L were performed by PCR-directed mutagenesis using pGEX5x-1-*h*NF-L as a template. Mutagenic primers for A148V are as follows: 5′-CTG CGC CTG G**T**G GCG GAA GAT-3′ (forward) and 5′-ATC TTC CGC C**A**C CAG GCG CAG-3′ (reverse); or mutagenic primers used for A296T: 5′-AAC ACC GAC **A**CC GTG CGC GCC-3′ (forward) and 5′-GGC GCG CAC GG**T** GTC GGT GTT-3′ (reverse). DNA sequencing using the dideoxy chain termination method confirmed that the desired substitutions were introduced at the appropriate codon to yield pGEX5x-1-*h*NF-L-A148V or - A296T.

Additional expression constructs

The EGFP-containing *h*NF-L expression plasmids were prepared by ligating pGEX5x-1-*h*NF-L or pGEX5x-1-*h*NF-L- A148V into EcoRI and SalI sites of pEGFP. Rat NF-M cDNA (rNF-M; kindly provided by Dr. Liem R. K. H., Columbia University) was ligated into the XbaI site of pREFA generating the expression plasmid, pREFA-*r*NF-M. All constructs were prepared using the Qiagen Plasmid Maxi Kit (Qiagen Inc., Santa Clarita, CA), and confirmed through direct sequencing of ligation junctions.

Cell culture

The vimentin-deficient (Vim^-) human adrenal carcinoma SW13 cell line was cultured in Dulbecco's Modified Eagles Media (DMEM) supplemented with 10% fetal bovine serum (FBS).

Analysis of intermediate filament formation

To study intermediate filament formation in mammalian cells,

*r*NF-M combined with either EGFP-*h*NF-L or EGFP-*h*NF-L-A148V fusion proteins were exogenously expressed in SW13 cells and examined using immunofluorescence microscopy. For transfections, SW13 cells were seeded onto glass coverslips in six-well plates, then co-transfected with pREFA-rNF-M and either pEGFP-*h*NF-L or pEGFP-*h*NF-L-A148V using a calcium phosphate co-precipitation kit (Promega, Madison, WI). Following transfection, cells were grown for 2 days in DMEM, then fixed at 37°C for 10 min in 4% paraformaldehyde and incubated with monoclonal anti-NF-M for 1 h at room temperature in a humidified chamber. The cells were washed with phosphate buffered saline (PBS), and then incubated with rhodamine-conjugated Affinipure goat anti-mouse IgG. Immunostained cells were observed using laser confocal microscopy.

Neurofilament-L protein purification

After *E.coli* (BL21) was transfected with a full-length cDNA clone of human NF-L in a pET-3d vector, bacteria was grown in a Luria broth containing 1 mM isopropyl β-Dthiogalactopyranoside at 37 for 3 h. Bacteria was harvested and resuspended in a standard buffer (50 mM MES, 170 mM NaCl, 1 mM DTT, pH 6.25). The cells were lysed with a French press at a pressure of 20,000 psi and centrifuged at 8,000 × g for 15 min at 4°C. The supernatant was incubated for 3 h at 37°C, then centrifuged at 100,000 × *g* for 20 min at 25°C. The aggregated NF-L proteins were washed twice with a standard buffer and dissolved in a urea buffer (25 mM Na-phosphate, pH 7.5, 6 M urea, 1 mM EGTA, and 1 mM DTT). The sample loaded onto a DEAE-Sepharose column was also washed with the urea buffer. The column was eluted with a linear 25-500 mM phosphate gradient in the urea buffer and the NF-L was eluted between 300 and 360 mM phosphate (31). The protein concentration was determined by the BCA method (32).

In vitro assay of NF-L self-assembly

Purified GST-NF-L-head (H), -rod (R), -tail (T), -head-rod (H/R) and head-rod-tail (F) domain fusion proteins were mixed with *E.coli*-purified native NF-L in Igepal buffer containing 1% bovine serum albumin, and incubated for 1 h at 4°C. The associated proteins were recovered by centrifugation, washed extensively, and analyzed by Western immunoblotting. Purified NF-L (2.5 μg) and the bead-bound GST-NF-L (H/R) fusion proteins (0.5 μg each) were incubated for 1 hr at 35°C. After extensive washing, the proteins bound to the beads were resolved by 10% SDS-PAGE and immunoblotted with anti-NF-L. The GST-NF-L- (H/R) bands with an anti-GST antibody represent the loading control.

Aknowledgements

This work was supported by Daejin University Research Grants.

REFERENCES

1. Lee, M.K., Xu, Z., Wong, P.C. and Cleveland, D.W. (1993) Neurofilaments are obligate heteropolymers *in vivo*. *J. Cell Biol.* **122**, 1337-1350.
2. Ching, G.Y. and Liem, R.K. (1993) Assembly of type IV neuronal intermediate filaments in nonneuronal cells in the absence of preexisting cytoplasmic intermediate filaments. *J. Cell Biol*. **122**, 1323-1335.
3. Nakagawa, T., Chen, J., Zhang, Z., Kanai, Y. and Hirokawa, N. (1995) Two distinct functions of the carboxyl-terminal tail domain of NF-M upon neurofilament assembly: cross-bridge formation and longitudinal elongation of filaments. *J. Cell Biol*. **129**, 411-429.
4. Al-Chalabi, A. and Miller, C.C. (2003) Neurofilaments and neurological disease. *Bioessays* **25**, 346-355.
5. Fuchs, E. and Weber, K. (1994) Intermediate filaments: structure, dynamics, function, and disease. *Annu. Rev. Biochem*. **63**, 345-382.
6. Grant, P. and Pant, H.C. (2000) Neurofilament protein synthesis and phosphorylation. *J. Neurocytol*. **29**, 843-872.
7. Pant, H.C. and Veeranna, V. (1995) Neurofilament phosphorylation. *Biochem. Cell Biol*. **73**, 575-592.
8. Nixon, R.A., Paskevich, P.A., Sihag, R.K. and Thayer, C.Y. (1994) Phosphorylation on carboxyl terminus domains of neurofilament proteins in retinal ganglion cell neurons *in vivo*: influences on regional neurofilament accumulation, interneurofilament spacing, and axon caliber. *J. Cell Biol*. **126**, 1031-1046.
9. Betts, J.C., Blackstock, W.P., Ward, M.A. and Anderton, B.H. (1997) Identification of phosphorylation sites on neurofilament proteins by nanoelectrospray mass spectrometry. *J. Biol. Chem*. **272**, 12922-12927.
10. Heins, S., Wong, P.C., Muller, S., Goldie, K., Cleveland, D.W. and Aebi, U. (1993) The rod domain of NF-L determines neurofilament architecture, whereas the end domains specify filament assembly and network formation. *J. Cell Biol*. **123**, 1517-1533.
11. Geisler, N. and Weber, K. (1981) Self-assembly *in vitro* of the 68,000 molecular weight component of the mammalian neurofilament triplet proteins into intermediate-sized filaments. *J. Mol. Biol*. **151**, 565-571.
12. Wong, P.C. and Cleveland, D.W. (1990) Characterization of dominant and recessive assembly-defective mutations in mouse neurofilament NF-M. *J. Cell Biol*. **111**, 1987-2003.
13. Monteiro, M.J., Hoffman, P.N., Gearhart, J.D. and Cleveland, D.W. (1990) Expression of NF-L in both neuronal and non-neuronal cells of transgenic mice: increased neurofilament density in axons without affecting caliber. *J. Cell Biol*. **111**, 1543-1557.
14. Herrmann, H. and Aebi, U. (2000) Intermediate filaments and their associates: multi-talented structural elements specifying cytoarchitecture and cytodynamics. *Curr. Opin. Cell Biol*. **12**, 79-90.
15. Lee, M.K. and Cleveland, D.W. (1996) Neuronal intermediate filaments. *Annu. Rev. Neurosci*. **19**, 187-217.
16. Choi, B.O., Lee, M.S., Shin, S.H., Hwang, J.H., Choi, K.G., Kim, W.K., Sunwoo, I.N., Kim, N.K. and Chung, K.W. (2004) Mutational analysis of PMP22, MPZ, GJB1, EGR2 and NEFL in Korean Charcot-Marie-Tooth neuropathy patients. *Hum. Mutat*. **24**, 185-186.

17. De Jonghe, P., Mersivanova, I., Nelis, E., Del Favero, J., Martin, J.J., Van Broeckhoven, C., Evgrafov, O. and Timmerman, V. (2001) Further evidence that neurofilament light chain gene mutations can cause Charcot-Marie-Tooth disease type 2E. *Ann. Neurol*. **49**, 245-249.
18. Fabrizi, G.M., Cavallaro, T., Angiari, C., Bertolasi, L., Cabrini, I., Ferrarini, M. and Rizzuto, N. (2004) Giant axon and neurofilament accumulation in Charcot- Marie-Tooth disease type 2E. *Neurologyo* **62**, 1429-1431.
19. Georgiou, D.M., Zidar, J., Korosec, M., Middleton, L.T., Kyriakides, T. and Christodoulou, K. (2002) A novel NF-L mutation Pro22Ser is associated with CMT2 in a large Slovenian family. *Neurogenetics* **4**, 93-96.
20. Jordanova, A., De Jonghe, P., Boerkoel, C.F., Takashima, H., De Vriendt, E., Ceuterick, C., Martin, J.J., Butler, I.J., Mancias, P. and Papasozomenos, S., et al. (2003) Mutations in the neurofilament light chain gene (NEFL) cause early onset severe Charcot-Marie-Tooth disease. *Brain* **126**, 590-597.
21. Mersiyanova, I.V., Perepelov, A.V., Polyakov, A.V., Sitnikov, V.F., Dadali, E.L., Oparin, R.B., Petrin, A.N. and Evgrafov, O.V. (2000) A new variant of Charcot-Marie-Tooth disease type 2 is probably the result of a mutation in the neurofilament-light gene. *Am. J. Hum. Genet*. **67**, 37-46.
22. Zuchner, S., Vorgerd, M., Sindern, E. and Schroder, J.M. (2004) The novel neurofilament light (NEFL) mutation Glu397Lys is associated with a clinically and morphologically heterogeneous type of Charcot-Marie-Tooth neuropathy. *Neuromuscul. Disord*. **14**, 147-157.
23. Gu, L., Troncoso, J.C., Wade, J.B. and Monteiro, M.J. (2004) *In vitro* assembly properties of mutant and chimeric intermediate filament proteins: insight into the function of sequences in the rod and end domains of IF. *Exp. Cell Res*. **298**, 249-261.
24. Carter, J., Gragerov, A., Konvicka, K., Elder, G., Weinstein, H. and Lazzarini, R.A. (1998) Neurofilament (NF) assembly; divergent characteristics of human and rodent NF-L subunits. *J. Biol. Chem*. **273**, 5101-5108.
25. Sarria, A.J., Nordeen, S.K. and Evans, R.M. (1990) Regulated expression of vimentin cDNA in cells in the presence and absence of a preexisting vimentin filament network. *J. Cell Biol*. **111**, 553-565.
26. Kim, S.K., Cho, S.M., Lee, I.B., Lee, Y.H., Kang, J.H., Choi, J.H., Suh, P.G. and Chang, J.S. (2007) *In vitro* assay of neurofilament light chain self-assembly using truncated mutants. *J. Neurosci. Methods* **161**, 199-204.
27. Sasaki, T., Gotow, T., Shiozaki, M., Sakaue, F., Saito, T., Julien, J.P., Uchiyama, Y. and Hisanaga, S. (2006) Aggregate formation and phosphorylation of neurofilament-L Pro22 Charcot-Marie-Tooth disease mutants. *Hum. Mol. Genet*. **15**, 943-952.
28. Levy, Y., Hanan, E., Solomon, B. and Becker, O.M. (2001) Helix-coil transition of PrP106-126: molecular dynamic study. *Proteins* **45**, 382-396.
29. Prusiner, S.B., Scott, M.R., DeArmond, S.J. and Cohen, F.E. (1998) Prion protein biology. *Cell* **93**, 337-348.
30. Inouye, H. and Kirschner, D.A. (1998) Polypeptide chain folding in the hydrophobic core of hamster scrapie prion: analysis by X-ray diffraction. *J. Struct. Biol*. **122**, 247-255.
31. Kim, N.H. and Kang, J.H. (2003) Oxidative modification of neurofilament-L by copper-catalyzed reaction. *J. Biochem. Mol. Biol*. **36**, 488-492.
32. Smith, P.K., Krohn, R.I., Hermanson, G.T., Mallia, A.K., Gartner, F.H., Provenzano, M.D., Fujimoto, E.K., Goeke, N.M., Olson, B.J. and Klenk, D.C. (1985) Measurement of protein using bicinchoninic acid. *Anal. Biochem*. **150**, 76-85.